Research Article

iMedPub Journals
http://www.imedpub.com

Polymer Sciences
ISSN 2471-9935

2017
Vol. 3 No. 1: 1

DOI: 10.4172/2471-9935.100016

Self-Assembly and Charge Transport of a Conjugated Polymer on ITO Substrates

Tanya M.S. David[1], Wondwosson Arasho[2], O'Neil Smith[3], Kunlun Hong[4], Carl Bonner[1,2] and Sam-Shajing Sun[1,2]

1 Center for Materials Research, Norfolk State University, 700 Park Ave, Norfolk, VA 23504, USA
2 Chemistry Department, Norfolk State University, 700 Park Ave., Norfolk, VA 23504, USA
3 Center for Organic Photonics and Electronics, School of Chemistry & Biochemistry, Georgia Institute of Technology, 901 Atlantic Dr., Atlanta, GA 30332, USA
4 Center for Nano phase Materials Science, Oak Ridge National Laboratory, P.O. Box 2008, Oak Ridge, TN 37832, USA

Corresponding author: Sun SS

ssun@nsu.edu

Chemistry Department, Norfolk State University, 700 Park Avenue, Norfolk, VA, USA.

Tel: +1-757-823-2993
Fax: +1-757-823-9054

Abstract

Conjugated oligomers and polymers are very attractive for potential future plastic electronic and opto-electronic device applications such as plastic photo detectors and solar cells, field effect transistors, and light emitting diodes. There are many desirable properties of conjugated polymers for opto-electronic devices such as flexibility and tenability, as well as their conductive property. Understanding and optimizing charge transport between an active polymer layer and conductive substrate is critical to the optimization of opto-electronic devices. This study focused on the design, synthesis, self-assembly, and electron transfers of conjugated polymers that are covalently attached to a conductive or semi-conductive substrate. Specifically, a phosphonic acid end-functionalized polyphenylenevinylene (PPV) was developed and self-assembled onto an Indium Tin Oxide (ITO) substrate. This study demonstrated how atomic force microscopy (AFM) can be an effective characterization technique in conjunction with conventional electron transfer rate study methods, including cyclic voltammetry (CV), towards determining electron transfer rate in polymer and polymer/conductor interface systems. This study found that the electron transfer rates of covalently attached and self-assembled films were much faster than the spin coated films. The knowledge from this study can be very useful for designing potential polymer based electronic and opto-electronic thin film devices.

Keywords: Conjugated polymers; Conducting substrates; Electrodes; Covalent attachment; Self-assembly; Electron transfer; Charge transport; Interface; Cyclic voltammetry

Received: January 27, 2017; **Accepted:** March 10, 2017; **Published:** March 23, 2017

Citation: David TMS, Arasho W, Smith O, et al. Self-Assembly and Charge Transport of a Conjugated Polymer on ITO Substrates. Polym Sci. 2017, 3:1.

Introduction

Self-assembly and covalent attachment of conjugated organic and polymeric materials on conducting substrates are essential for the development of future generation polymer based electronic and optoelectronic devices, and electron transfers between organic or polymeric species and electrodes are also essential [1-4]. There are a number of methods used to measure electron transfer between the organic species and the conducting substrate, for example, Voltammetric or impedance-based methods [5,6]. Cyclic voltammetry (CV) is an oxidation and reduction method that used to measure the kinetics of charge injection between a contact electrode and the organic material [7]. This method is versatile, low cost, and is accompanied by multitude of theoretical and experimental literature. Using this method, redox species like ferrocene and ferricyanide have been shown to undergo a reversible one-electron transfer process, from which electron transfer rate can be determined using the Laviron equations [8]. CV has also been used to determine the Electroactive surface coverage (Nk or Γ) using an electrochemical reaction expression (discussed later in this paper) [9,10]. Even though these methods (CV, Laviron equation, and electrochemical reaction expression) are widely used, we believe that due to its high spatial resolution, atomic force microscopy (AFM) can quantitatively provide an accurate description of the topographic coverage of the polymer on the substrate's surface, interacting with the working electrode in an electrochemical cell. AFM can measure the height and cross-section of individual polymer

chains or clusters. The resolution of the technique can be used to determine the fractional coverage of the electrode. It is this scaled coverage, which can be used to identify the percentage of bonded species that can contribute to the transport of electrons and the overall electron transfer rate. Conventional Atomic Force Microscopy is a scanning probe microscope that can measure properties of a surface such as height, friction, and magnetism [11]. AFM analysis of a substrate can provide important information such as surface roughness, grain height, particle size, and surface coverage based on particle height and size. This collection of AFM information is usually reported in articles mainly for morphological studies of a surface and not as a method to assist in calculating Electroactive coverage or electron transfer rate. Here in this paper we report a new approach and method of determining the electron transfer rates using a combination of cyclic voltammetry, atomic force microscopy, the Laviron method, and electrode kinetic calculations. Assembly of organic species on conducting substrates in the form of molecular wires and molecular assemblies have been widely studied, and within recent years, research have increased in polymer assemblies on varies conducting substrate [3,4,12]. Conjugated polymers end-functionalized with phosphonic acid anchoring groups have been grafted onto oxide substrates such as indium tin oxide (ITO) [5,13-16], zinc oxide [17], silicon dioxide (SiO_2) [18], titanium dioxide (TiO_2) [19,20], and aluminium oxide (Al_2O_3) [21]. Through a dehydration (condensation) reaction, the phosphonic acid group binds to each substrate covalently and possibly electrostatically (via hydrogen bonds), producing several binding modes [15]. Even though covalent binding of phosphonic acid end-functionalized polymers onto conducting substrates have been reported, there have been no reports studying electron transfer rate of polymeric materials with both CV and AFM as quantitative analysis methods. A particular phosphonic acid end-functionalized Poly (1, 4-phenylenevinylene-alt-[2,5-Bis-(2-ethyhexyloxy)]-p-phenylenevinylene) or P (PEH-PPV) was used for these studies, and the synthesis are described. A "grafting-to" approach was used to graft the phosponic acid end-functionalized polymer onto Indium Tin Oxide (ITO) substrates. Subsequent characterization methods for covalent self-assembly and charge transport will be described and discussed in detail.

Experimental

Instrumentation

Proton and Carbon NMR spectra were recorded at a 300 MHz NMR spectrometer with TMS as an internal reference. UV-Vis absorption data were collected on a Perkin-Elmer Lambda 900 Spectrophotometer. Atomic force microscopy images were done on a Veeco Dimension Icon in tapping mode using a 300 kHz Silicon tip with a 40 N/m force constant, and a 5 um × 5 um scan area. AFM data analysis was conducted using a Nano scope Analysis version 1.40 by Brucker. Electrochemical studies (cyclic voltammetry) were performed on a CH Instruments Potentiostat (CH1030A) using the conventional three-electrode configuration. Tetrabutylammonium hexafluorophosphate (TBA HFP) (0.1 M) in acetonitrile was used as the supporting electrolyte. Ag/$AgNO_3$, Pt wire, Al and ITO were used as the reference electrode, counter electrode and working electrode, respectively. ITO is also considered a working electrode since the polymer was sandwiched between ITO and the Al. Ferrocene (2 mm in 0.10 M TBA-HFP/ CH_3CN solution) was used as an internal reference standard, and was tested with pristine ITO/Al, Pt wire, and glass carbon to check for system errors. Before starting a measurement, dry nitrogen gas was bubbled through the anhydrous solvents for at least 10 min to remove any dissolved oxygen. Between the experiments, the surface of the electrodes were cleaned and polished. Scan rate was 0.1 V/s. CV graph analysis was conducted using CH Instruments Inc. (CHI420A version 10.09) processing program to obtain standard CV variables such as the peak current (Ip), peak potential (Ep), and charge (Q).

Conversion of PEH-PPV phosphonate to phosphonic acid: In a 25 ml round bottom flask equipped with a stirring bar, 1 ml of THF was added to 20 to 30 mg of diphosphonate polymer, and the polymer was allowed to dissolve. 8 M HCl in EtOH was then added to the mixture, and the solution was heated between 70°C to 75°C for three to five days. The phosphonate/phosphonic acid polymer mixture was collected by filtration, washed with distilled H_2O and MeOH, and dried in vacuo. Yield was ~40-60%. ^1H NMR ($CDCl_3$): δ (ppm) 0.95-1.03 (m, H), 1.25-1.68 (m, H), 1.85 (t, J=5.97 Hz, H), 3.44 (t, J=6.16 Hz, H), 3.57 (t, J=6.64 Hz, H), 3.98 (d, J=4.61 Hz, H), 7.14 (d, J=15.93 Hz, H), 7.53 (t, J=8.76 Hz, H) 9.99 (s), 10.46 (s). ^{13}C NMR ($CDCl_3$): δ (ppm) 11.39, 14.18, 23.17, 24.29, 29.33, 31.01, 39.82, 71.85, 110.22, 126.83, 151.4.

Polymer solution preparation: PPV phosphonic acid polymer (4.6×10^{-4} M) was placed in a 20 ml vial cleaned by a 10 sec piranha bath, DI water rinse, 10 min sonication with ethanol, ethanol rinse, and dried with N_2. The polymer was gently heated in 1 ml of THF to fully dissolve the polymer. Ethanol was added to the solution (a few drops to 0.5 ml) to promote binding.

Substrate preparation: Indium Tin Oxide glass slides were purchased from Delta Technologies LTD and were cut into 1" × 1" pieces. These pieces were cleaned by sonication in detergent (10 min), deionized (DI) water twice (10 min each) and ethanol (10 min), and dried under a stream of nitrogen. The substrate was subjected to ozone treatment at 140°C for 20 min or plasma etching for 10 minutes under a gentle flow of oxygen, and was immediately placed in a clean vial with the polymer solution.

Self-assembly: The cleaned ITO substrates were immersed in the polymer solution, and the vials were tightly sealed. The self-assembly formation was carried out for 24-48 hrs., and then annealed at 130°C for 1 hr to convert surface-absorbed phosphonic acid to surface-bound phosphonate [6,22].

The substrate was sonicated in $CHCl_3$ (3 min), rinsed with $CHCl_3$, sonicated with THF (1 min), rinsed with THF, and N_2 dried. Some substrates were sonicated in heated CHCl3 (40°C) for 10 min as to ensure any unbound polymer phosphonic acid was removed.

Results/Discussion

Synthesis

Different molarities of HCl/EtOH solutions (2 M, 3 M, 6 M, and 8 M) were used to determine which concentration of HCl can

more effectively hydrolyzed the phosphonate group (– P(O) OCH_2CH_3) without hydrolyzing the alkoxy substituents on the PPV monomer. Each reaction was repeated several times as to ensure the reliability and reproducibility of the results. 8 M HCl/EtOH solutions were the only molarity that produced a mixture of unconverted phosphonate, mono phosphonic acid/phosphonate, and potentially diphosphonic acid end-functionalization. **Scheme 1** shows the hydrolysis reaction with what is believed to be the major phosphonic acid product, mono phosphonic acid/phosphonate end-functionalized. 2 M, 3 M, and 6 M HCl solutions all gave starting material, even when heated up to 80°C for 5 to 6 days. 10 M HCl/EtOH solutions were attempted but gave complete degradation of the monomer, and therefore were not included in the trial. It should be noted that experiments using traditional reagent that is known to hydrolyzed the phosphonate group, iodo trimethylsilane ($(CH_3)3SiI$) and sodium iodide (NaI), were also attempted but resulted in unwanted and inseparable side products. Since 8 M HCl/ethanol solutions gave the most promising hydrolysis of the monomer unit, it was used for the conversion of PEH-PPV diphosphonate polymer to phosphonic acid. The conversion yield of the monomer was factored into the probable yield for the conversion for the polymer; approximately 40% based on ^1H NMR analysis. Gel Permeation Chromatography (GPC) of the polymer sample indicated a polydispersed polymer (PDI of 3.5) with an average molecular weight of approximately 6564 Daltons, which corresponds to polymers chains of approximately 14 repeat units in length. However, given the polydisperse nature of the polymer, the polymer chains can range from ~10 to ~30 repeat units with each monomer unit being ~1.3 nm length [23].

UV-visible spectroscopy

UV-Visible Spectroscopy was the first preliminary method of characterization, to determine if the PPV polymer adhered to the surface. As shown in **Figure 1**, a UV-Vis spectrum was taken of the polymer coated ITO after the assembly process but before an initial washing. Two separate washing processes were used, each to demonstrate that the self-assembly did occur and that there are no layer-by-layer assemblies on the substrate. The sample used in the UV-Vis spectra shown in **Figure 1** underwent the most vigorous washing process; sonicated in $CHCl_3$ for 10 minutes at 40°C, rinse with $CHCl_3$, and dried under a stream of nitrogen. This process was repeated three more times, and UV-Vis absorption was taken after each washing process. After the first wash there was very little difference in the amount of polymer that remained attached to the substrate during the remaining washes. As can be seen there was still a measured absorption for each sample, indicating that the self-assembly was successful. The λmax for PPV in solution and self-assembly is 466 nm.The polymer covered ITO appeared yellow in color. This data provided good preliminary evidence that the polymer covalently bonded to the ITO surface. As a comparison, for spin coated polymer films, one $CHCl_3$ wash would completely remove the polymer sample without any absorption residue.

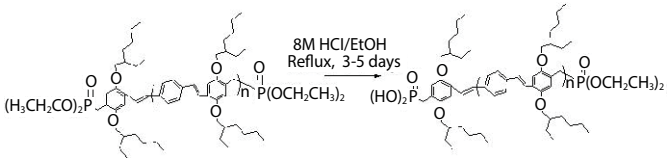

Scheme 1 UV-Vis spectrum of unwashed ITO slides after self-assembled with phosphonic acid functionalized PPV polymer, and after four subsequent sonication and washes with chloroform.

Atomic force microscopy

AFM was not only used to confirm the presence of polymeric structures on the surface of the ITO, but to also distinguish between pristine ITO, PPV polymer spin coated on ITO, and covalently bond polymeric structures on the ITO. AFM was also used to quantitatively determine the number of polymeric structures bonded to the surface of ITO and the area coverage on the substrate's surface. The same concentration of the polymer solution used for self-assembly (4.6×10^{-4} M) was used for the spin coated sample. **Table 1** shows the AFM images of pure ITO (a), ITO with spin coated PPV polymer (b), and ITO with PPV polymer structures bonded to the ITO surface (c). The AFM showed that the root-mean-square (RMS) roughness for pure ITO was 2.65 nm.

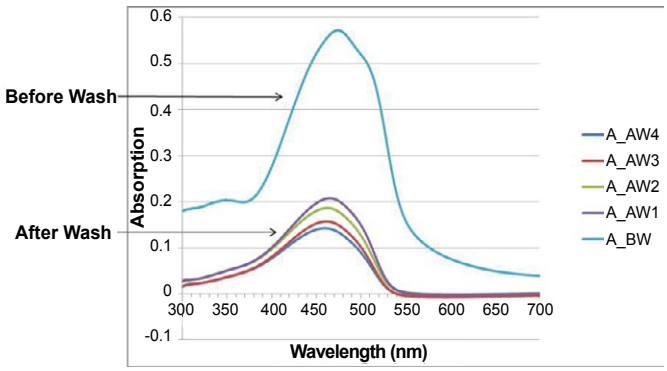

Figure 1 UV-Vis spectrum of unwashed ITO slides after self-assembled with phosphonic acid functionalized PPV polymer, and after four subsequent sonication and washes with chloroform.

Table 1: AFM images of pristine ITO (a), ITO with spin coated PPV polymer (b), and ITO with PPV polymer structures bonded to the ITO surface (c), as well as corresponding RMS and cross sectional height of each.

	a	b	c
	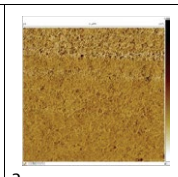	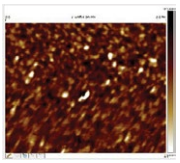	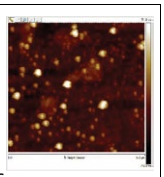
	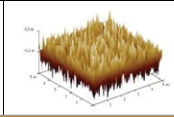	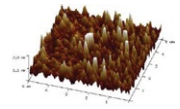	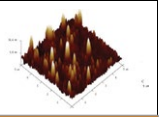
Rms	2.65 nm	1.82 nm	5.74 nm
Cross Section Height	5.9 nm	5-8 nm	5-40 nm

The ITO with spin coated PPV polymer showed a much smoother surface with an RMS of 1.82, and in contrast, the ITO with the polymer-assembled on ITO surface had an RMS of 5.74 (rougher than both pure ITO and spin coated samples). Cross sectional analysis showed grain heights of 5-9 nm for both pure ITO and spin coated PPV on ITO, but grain height ranging from 5 to 40 nm for the polymer-assembled on ITO. Given the very "grainy" or "hills-and-valleys" nature of the ITO, it is hypothesized that the polymer structures, which has a varying distribution in height, assembled around the rigid non-uniform structure of the ITO's surface to create a similar "hills-and-valleys" pattern.

In an effort to distinguish between structure height due to ITO grains, polymer-assembled structures, or a combination of both, particle threshold height and depth analysis were conducted. Using the ITO RMS of 2.5 nm, particle analysis was done on each AFM image to determine the number of particles (which includes ITO grains and polymeric structures) and particle area at the threshold height of pure ITO (2.5 nm), two times the ITO RMS height (5.3 nm), and three times the ITO RMS height (7.95 nm). This data is summarized in **Table 2**. According to the analysis, more than half the polymer-assembled structures (163) were three times higher than the RMS value of bare ITO, whereas only 14 of the original 2063 particles on the bare ITO was three times higher than the RMS. If only the grain heights (particle heights) above 7.95 nm (three times the ITO RMS value) were used to determine polymer structure length, given that each monomer unit length is ~1.3 nm, the polymer-assembled structures would have polymer chain lengths that ranged from 6 to 30 repeat units. This is in reasonable accordance with the repeat units determined by GPC. As shown the particle area was also much larger, indicating that there were not only particles covering large areas of the ITO surface but also, that these structures were in fact at a significant height, up to 40 nm according to cross sectional analysis. **Figure 2** shows the phase images of the particles, appearing blue, at two times the threshold height of ITO RMS height (5.3 nm). As shown, there are more particles twice the height of the RMS value for the ITO with the polymer-assembled structures than the spin coated and pure ITO. To reflect, the polymer-assembled ITO samples were vigorously sonicated and washed to ensure no layer-by-layer interaction was present. However, due to the larger clusters of polymers structures on the ITO surface, it is believed that polymers assembled in clusters around the ITO "hills and valleys" grains, versus evenly dispersed assembles. This assembly pattern could be due to any number of reasons including, absorbate concentration, formation of polymer brushes, and reactivity of binding sites [13,24]. The particle count and particle area for twice the threshold height (5.3 nm) was used to calculate the Electroactive surface coverage. One assumption that was made when analysing the images using AFM was that a practical minimum detectable height of surface features that could be attributed to a polymer chain (or cluster) would be twice the RMS surface roughness (5.3 nm) of bare ITO. This would require the chain be longer than the height of the deepest surface valley. This model does not account for the possibility of the polymer tilting relative to the surface normal. If the effect of tilting was included, the threshold limit could have been lower which, would in turn result in a higher coverage area.GPC was used to set the threshold surface feature height that was used to discriminate between the bare ITO surface and any polymer that was attached to the surface. From GPC measurements of the polymer molecular weight, the average polymer molecular weight (6564 Daltons) which corresponds to polymers chains of approximately 14 repeat units that is 18 nm in length. Given the wide polydispersity of the polymer, it was assumed that setting the threshold limit of 5.3 nm (twice the rms surface roughness of the bare ITO) should be more than sufficient to identify the presence of polymer chains on the ITO surface. It should be noted however that, with the wide polydispersity, it is possible for there to be bonded polymer chains with lengths shorter the 18 nm that do not meet this detection threshold as well as polymers that may be bonded in the undulations (valleys) of the ITO surface that do not protrude above the rms surface roughness.

Table 2: Particle threshold height and particle area at the threshold height of pure ITO (2.5nm), two times the ITO RMS height (5.3 nm), and three times the ITO RMS height (7.95 nm) for pristine ITO, spin coated PPV on ITO, and covalently bonded PPV on ITO.

	Threshold Height: 2.65 nm		Threshold Height: 5.3 nm (2x ITO RMS)		Threshold Height: 7.95nm (3x ITO RMS)	
	Particle Count	Particle Area (nm^2)	Particle Count	Particle Area (nm^2)	Particle Count	Particle Area (nm^2)
Pristine ITO	2063	1935	548	534	14	1355
Spin Coated PPV	155	9984	28	10299	10	10070
Covalently Bonded PPV	328	15609	249	12368	163	11889

Cyclic voltammetry

Figure 3 shows the comparative CV of the covalently bonded PPV thin film (solid line) versus the spin coated thin film (dashed line) when initially oxidized (positive potential (E)). As the data show, both graphs have two oxidation peaks but only one much smaller reduction peak. This means: 1) there was a two-electron transfer from the polymer to the ITO/Al, but only a one-electron transfer from the ITO/Al back to the polymer, and 2) that not all of the electrons were transferred back to the polymer given the

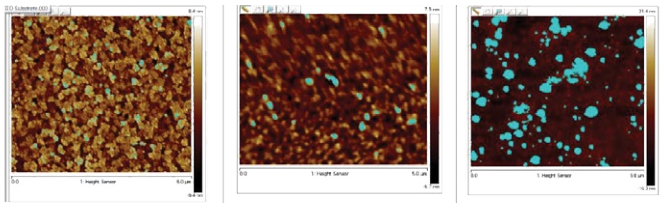

Figure 2 AFM phase images of the particles, appearing blue, at two times the threshold height of ITO RMS height (5.3 nm) for pristine ITO (a), spin coated PPV on ITO (b), and covalently bonded PPV on ITO (c).

size of the reduction peak. The redox reaction is not considered totally irreversible, but it is non-symmetrical for both spin coated thin films and covalently bonded PPV thin films. **Figure 3** shows what appears to be a one-electron transfer in both redox states, where the second oxidation peak at ~0.1 V is attributed to the possible change of chemical composition of the polymer since the polymer starts to decompose. Decomposition could also be observed in physical changes of the polymer, such as the polymer changing from a THF soluble yellowish-orange polymer film to a THF insoluble black residue. Decomposition occurs in both spin coated and covalently bonded PPV thin film when initially reduced (negative potential). No decomposition occurs when the polymer initially undergoes positive potential (initially oxidized), however as seen in the eight-segment cycle scan in **Figure 4**, the covalently bonded PPV polymer transitions from a chemisorb state to a physisorb after the first cycle (solid line). Then, the physisorption interaction is further weakened after the completion of each cycle, until the polymer is completely

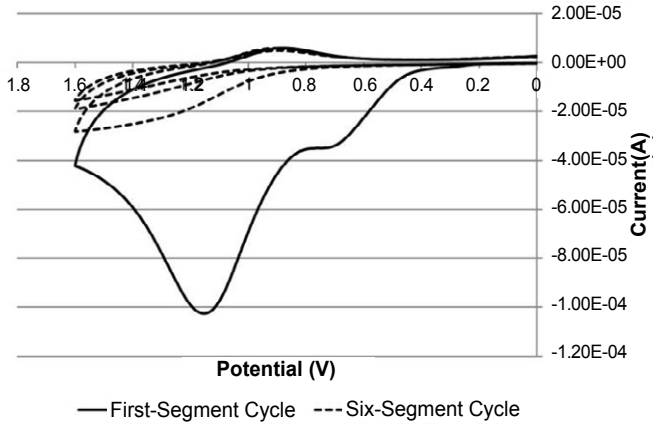

Figure 3 CV of the covalently bonded PPV thin film (solid line) versus the spin coated thin film (dashed line) when initially oxidized (positive potential (E)).

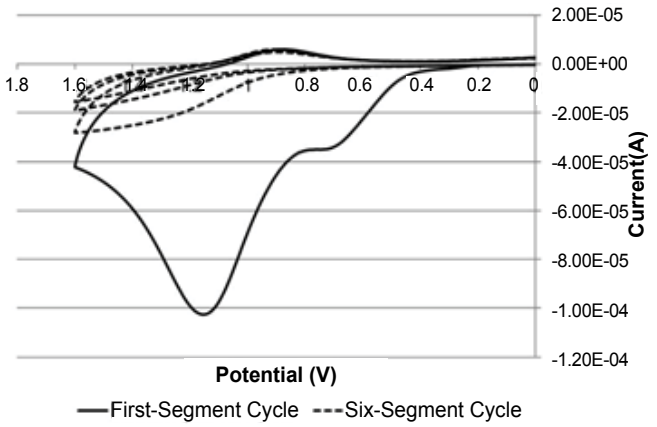

Figure 4 Eight-segment cycle scan for the covalently bonded PPV; where the first cycle (solid line) shows the transitions from a chemisorb state to a physisorb state in the remaining six cycles (dashed lines).

removed (dashed line). It appears that the applied electrical energy was much larger than the binding energy of the P-O-M bonding energy, and cleaves the P-O-M bond after the redox cycle. To calculate the electron transfer rate constants, only the first (large) oxidation peak with max potential at ~1.14 V, and the corresponding reduction peak at ~1.02 V were used, since this is the only reversible redox process. The smaller oxidation peak at ~0.68 V was not used.

Electron transfer rate determined from AFM and CV

Atomic Force Microscopy and Cyclic Voltammetry were used to determine the rate of electron transfer along the P (PEH-PPV) backbone. A series of equations was used to help calculate the electron transfer rate. The unimolecular rate constant ks (for species chemically anchored to the surface of a substrate) was calculated using the well-known Laviron equation shown in equation 1 [8].

$$\log k_s = \alpha \log(1-\alpha) + (1-\alpha) + (1-\alpha)\log\alpha - \log\frac{RT}{nF\nu} - \alpha(1-\alpha)nF\frac{E-E_0}{2.3RT} \quad (1)$$

Where n is the number of electrons required for oxidation of a single conjugated chain, F is Faraday's constant, R is the molar gas constant, T is the temperature, E is applied potential, E^0 is formal potential, and α is the cathodic electron transfer coefficient.[8] In traditional symmetrical redox reactions there are a few things that are assumed in calculating the ks: 1) alpha is assumed to be 0.5 for symmetric one-electron transfer redox process, and 2) the change in potential is usually plotted versus the change in scan rate and from a linear fit line another variable (m) is calculated. From other equations not shown in this paper, m can be used to calculate the rate of electron transfer (Tafel Plot [8]). However, since the redox reaction for PPV polymer systems on ITO were not symmetrical, alpha had to be calculated. As shown in **Figure 5**, by integrating the area under the reduction and oxidation potential curves, the peak current (Ip), peak potential (Ep), and charge (Q) can be determined using a CV processing program, and the values used to calculate the algebraic scan rate (v) for each redox potential using equation 2 [25].

$$\nu_{a\,or\,b} = \frac{I_p * E_p}{6.24*10^{18}} \quad (2)$$

Given the relation between alpha and the Red/Ox scan rate shown in Equation 3, alpha was calculated to be 0.959 for the covalently bond PPV and 0.989 for the spin coated PPV. The high alpha values indicate that the transition state for electron transfer is closer to the oxidation state [7]. Once alpha was calculated, equation 1 was used to calculate ks (s^{-1}) [8]. As shown in **Table 3** the ks for covalently bonded PPV polymer is an order of magnitude larger (5.24×10^{-1} s^{-1}) than that of spin coated PPV polymer on ITO (4.98×10^{-2} s^{-1}). This is believed to be due to the strong intermolecular charge transport between the ITO substrate and the covalently bonded PPV.

$$\log\left[\frac{\alpha}{1-\alpha}\right] = \log\left(\frac{\nu_a}{\nu_b}\right) \rightarrow \alpha = \frac{\nu_a}{\nu_b+\nu_a} \quad (3)$$

Conventionally the Electroactive surface coverage, Nk (or also seen as Γ with units mol cm^{-2}), which is the total charge of bonded

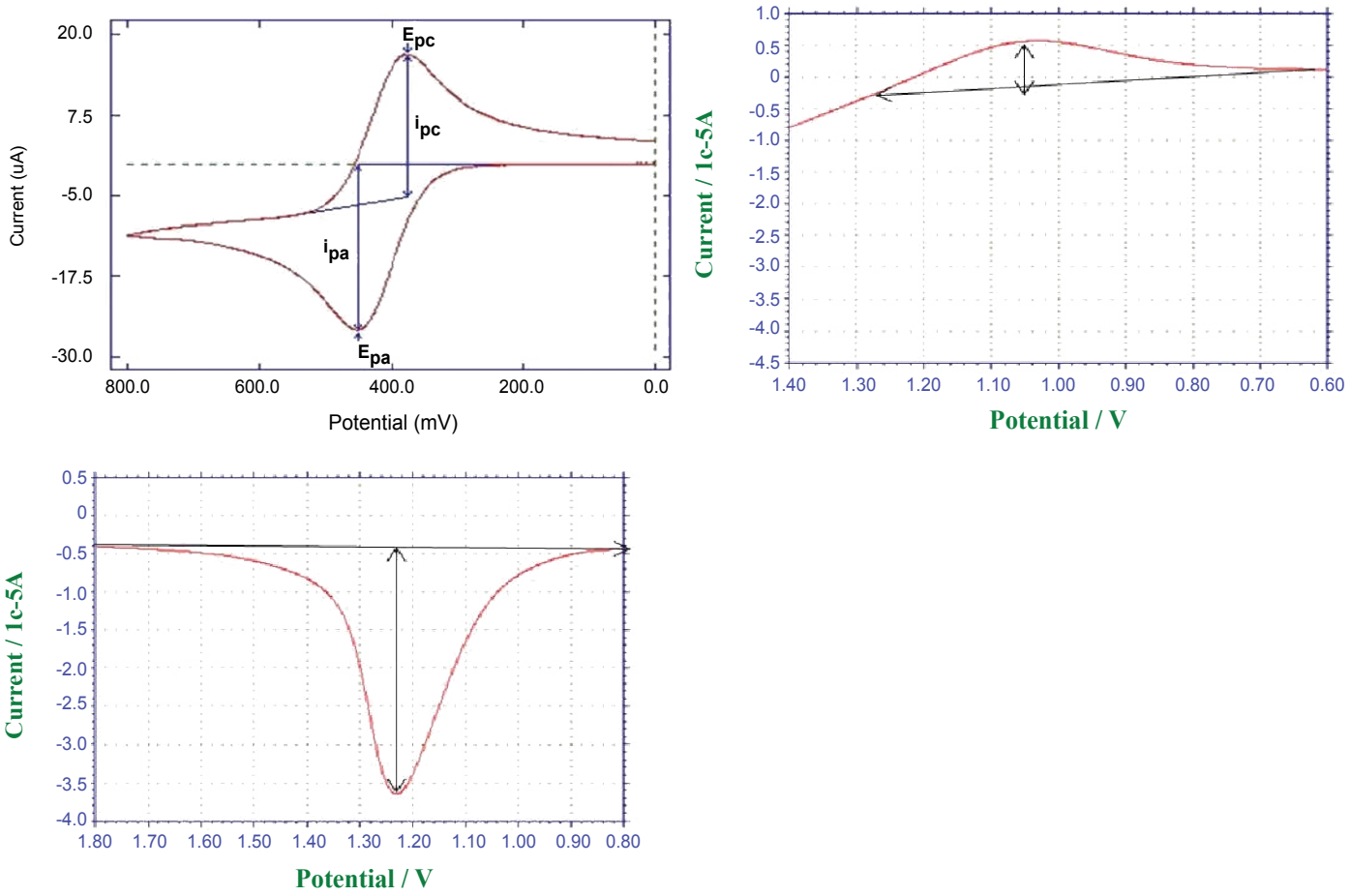

Figure 5 Examples of integrating the area under the reduction and oxidation potential curves to obtain peak current (Ip), peak potential (Ep), and charge (Q).

species per unit electrode area, is calculated using Equation 4. Where, Q is the average charge required for the redox process, n is the number of electrons required for oxidation of a single conjugated chain, F is Faraday's constant, and A is usually the electrode area (tested area). The value of n is either 1 or 2 depending on the number of peaks which is equivalent to the number of electrons transferred (i.e. n=1=1 electron transfer) [9,10].

$$N_k = \frac{Q}{nFA} \quad or \quad Q = nFAN_k \tag{4}$$

However, we believe that this equation alone does not give an accurate percentage of bonded species that contribute to the transport of electrons. In an effort to quantitatively and experimentally determine the number of bonded species on the surface of the electrode, the percent of surface coverage, as well as the rate of electron transfer through the polymeric backbone of the polymer structure, a combination of AFM and a further derived version of equation 4 were used. AFM was used to determine polymer structure count and polymer coverage area on the ITO surface. Using the particle area at twice the RMS height of pristine ITO (5.3 nm) for both spin coated and covalently bonded PPV, the polymer coverage for a 25 µm AFM scan area was 41.2% and 49.5% respectively. Utilizing this fractional polymer coverage for a 25 µm AFM scan area, the polymer coverage for the electrode cell area (0.6723 cm^2) was calculated to be 27.7% and 33.2% for spin coated and covalently bonded PPV, respectively. Factoring this polymer coverage as the actual contributing polymer area as A in equation 4 the Electroactive surface coverage, Nk, was calculated as 1.31×10^{-10} mol cm^{-2} and 1.41×10^{-11} mol cm^{-2} for spin coated and covalently bonded PPV, respectively (**Table 3**). This is in comparison to 7.82×10^{-9} mol cm^{-2} and 7.0×10^{-10} mol cm^{-2} if the cell area (test area) of 0.6723 cm^2 was used to calculate the Electroactive area. We believe that the AFM provides a more quantitative and realistic viewpoint of the Electroactive area. It should be noted that since Nk, which is the total charge of bonded species per unit electrode area, is based on measured current these calculations are insensitive to molecules bonded to an inactive site. Equations 5 and 6 shows the relationship between the Nk (mol cm^{-2}), unimolecular rate constant ks (s^{-1}), and the heterogeneous electrochemical rate constant (or the observed rate constant along the polymer backbone) KE' (cm s^{-1}) where ao is the interfacial concentration of reactant species (with units of mol cm^{-3}) [26]. The interfacial concentration of reactant species ao is calculated from the Nk divided by the average polymer chain length which is determined

Table 3: Combined AFM and CV characteristics of covalently bonded PPV and spin coated PPV on ITO.

	Ks (s^{-1})	% Cell Cov (0.6723 cm^2)	Avg. Charge	Nk (mol cm^{-2})	Ao (mol cm^{-3})	kE′ (cm s^{-1})
Spin Coated Polymer	$4.98 \times 10^{-2} \pm 0.02$	27.7%	3.49×10^{-4}	1.31×10^{-10}	7.18×10^{-5}	$9.06 \times 10^{-8} \pm 1 \times 10^{-23}$
Covalently Bonded	$5.24 \times 10^{-1} \pm 0.1$	33.2%	4.54×10^{-5}	1.41×10^{-11}	7.77×10^{-6}	$9.53 \times 10^{-7} \pm 1 \times 10^{-22}$

by gel permeation chromatography. As discussed previously, the polymer-assembled structures covalently bonded to the ITO would have polymer chain lengths that ranged from 6 to 30 repeat units. The average polymer chain length corresponding to 14 repeat units (18.2 nm or 1.82×10^{-6} cm), obtained from GPC, was used to calculate the interfacial concentration of reactant species, ao. Even though for 14 repeat units, spin coated and covalently bonded PPV had values of 7.18×10^{-5} mol cm^{-3} and 7.77×10^{-6} mol cm^{-3}, respectively, these values could range in correspondence to the range in structure size or polymer chain length (7.95 nm to 40 nm**)** (Equations 5 and 6).

$$a_0 = \frac{N_k}{avg\ polymer\ chain\ length} \quad (5)$$

$$k'_E = \frac{k_S * N_k}{a_0} \quad (6)$$

This range in polymer chain length can of course also affect the electron transfer rate along the polymer backbone, kE′. However, even though not shown in **Table 3**, no matter the chain length, the electron transfer rate along the polymer backbone in the covalently bonded PPV polymer is an order of magnitude faster (9.53×10^{-7} cm s^{-1}) than spin coated PPV (9.06×10^{-8} cm s^{-1}).

Conclusion

Self-assembly and covalent attachment of conjugated PEH-PPV on conducting ITO substrate were characterized by UV-Visible absorption spectroscopy, atomic force microscopy (AFM), and cyclic voltammetry (CV). This study demonstrates the effectiveness and the important contribution that AFM can play in determining not only polymer self-assembly coverage on a conducting substrate, it also provide a more quantitative analysis for electron transfer rates in similar systems. Specifically, this study shows the average electron transfer rate along the polymer backbones in the covalently bonded PPV polymer on ITO is an order of magnitude faster (9.53×10^{-7} cm s^{-1}) than spin coated PPV (9.06×10^{-8} cm s^{-1}). The redox process of PEH-PPV is only slightly reversible with a one electron transfer process. Through data analysis of the AFM images of the pristine ITO, spin coated PEH-PPV on ITO, and covalently bonded PEH-PPV on ITO, the covalent attachments of conjugated polymers on ITO substrate was confirmed to range from about 7.95 nm to 40 nm (corresponding to 6 to 30 repeat units). Particle area data obtained from the AFM used in conjunction with the conventional Laviron method showed that the Electroactive surface coverage, Nk, was calculated as 1.31×10^{-10} mol cm^{-2} and 1.41×10^{-11} mol cm^{-2} for spin coated and covalently bonded PPV, respectively. From this information, a more quantitative analysis of the electron transfer rate in the polymer backbone could be determined.

Acknowledgement

We would like to thank Dr. Aswini Pradhan and Mr. Brandon Walker for assistance on AFM measurements. This material is based upon work supported, in part, by research and educational grant awards from a number of sponsors including the Department of Energy (DOE Award # DE-EE-0004002), Army Research Office (ARO Award # W911NF-15-1-0422), and the National Science Foundation (NSF Award # 1036494 and HRD-1547771).

References

1 McCreery RL (2004) Molecular Electronic Junctions. Chem Mater 16: 4477-4496.

2 McCreery RL, Bergren AJ (2009) Progress with Molecular Electronic Junctions: Meeting Experimental Challenges in Design and Fabrication. Adv Mater 21: 4303-4322.

3 Miozzo L, Yassar A, Horowitz G (2010) Surface Engineering for High Performance Organic Electronic Devices: The Chemical Approach. J Mater Chem 20: 2513.

4 Bousquet A, Awada H, Hiorns RC, Dagron-Lartigau C, Billon L (2014) Conjugated-Polymer Grafting on Inorganic and Organic Substrates: A New Trend in Organic Electronic Materials. Prog Polym Sci 39: 1847-1877.

5 Doubina N, Jenkins JL, Paniagua SA, Mazzio KA, MacDonald GA, et al. (2012) Surface-Initiated Synthesis of Poly(3-Methylthiophene) from Indium Tin Oxide and Its Electrochemical Properties. Langmuir 28: 1900-1908.

6 Bardecker JA, Ma H, Kim T, Huang F, Liu MS, et al. (2008) Self-Assembled Electroactive Phosphonic Acids on ITO: Maximizing Hole-Injection in Polymer Light-Emitting Diodes. Adv. Funct Mater 18: 3964-3971.

7 Bond AM (2003) Broadening Electrochemical Horizons: Principles and Illustration of Voltammetric and Related Techniques; Oxford University Press: Oxford , New York.

8 Laviron E (1979) General Expression of the Linear Potential Sweep Voltammogram in the Case of Diffusionless Electrochemical Systems. J Electroanal Chem 101: 19-28.

9 Li J, Wang L, Liu J, Evmenenko G, Dutta P, et al. (2008) Characterization of Transparent Conducting Oxide Surfaces Using Self-Assembled Electroactive Monolayers. Langmuir 24: 5755-5765.

10 Wang J (2004) Analytical Electrochemistry. John Wiley & Sons.

11 Duwez AS, Willet N (2011) Molecular Manipulation with Atomic Force Microscopy; CRC Press.

12 Tour JM (1996) Conjugated Macromolecules of Precise Length and Constitution. Organic Synthesis for the Construction of Nano architectures. Chem Rev 96: 537-554.

13 Hotchkiss PJ, Jones SC, Paniagua SA, Sharma A, Kippelen B, et al. (2012) The Modification of Indium Tin Oxide with Phosphonic Acids: Mechanism of Binding, Tuning of Surface Properties, and Potential for Use in Organic Electronic Applications. Acc Chem Res 45: 337-346.

14 Paniagua SA, Hotchkiss PJ, Jones SC, Marder SR, Mudalige A, et al. (2008) Phosphonic Acid Modification of Indium–Tin Oxide Electrodes: Combined XPS/UPS/Contact Angle Studies. J Phys Chem C 112: 7809-7817.

15 Paramonov PB, Paniagua SA, Hotchkiss PJ, Jones SC, Armstrong, NR, et al. (2008)Theoretical Characterization of the Indium Tin Oxide Surface and of Its Binding Sites for Adsorption of Phosphonic Acid Monolayers. Chem Mater 20: 5131-5133.

16 Feng G (2012) the Synthesis and Characterization of Phosphonic Acids for the Surface Modification Study on Indium Tin Oxide. Dissertation, Georgia Institute of Technology.

17 Briseno AL, Holcombe TW, Boukai AI, Garnett EC, Shelton SW et al (2010) Oligo- and Polythiophene/ZnO Hybrid Nanowire Solar Cells. Nano Lett 10: 334-340.

18 Hanson EL, Schwartz J, Nickel B, Koch N, Danisman MF (2003) Bonding Self-Assembled, Compact Organophosphonate Monolayers to the Native Oxide Surface of Silicon. J Am Chem Soc 125: 16074-16080.

19 Gawalt ES, Avaltroni MJ, Koch N, Schwartz J (2001) Self-Assembly and Bonding of Alkanephosphonic Acids on the Native Oxide Surface of Titanium. Langmuir 17: 5736-5738.

20 Guerrero G, Mutin, PH, Vioux A (2001) Anchoring of Phosphonate and Phosphinate Coupling Molecules on Titania Particles. Chem Mater 13: 4367-4373.

21 Pellerite MJ, Dunbar TD, Boardman LD, Wood EJ (2003) Effects of Fluorination on Self-Assembled Monolayer Formation from Alkanephosphonic Acids on Aluminum: Kinetics and Structure. J Phys Chem B 107: 11726-11736.

22 Hanson EL, Guo J, Koch N, Schwartz J, Bernasek, SL (2005) Advanced Surface Modification of Indium Tin Oxide for Improved Charge Injection in Organic Devices. J Am Chem Soc 127: 10058-10062.

23 Fried JR (2014) Polymer Science and Technology; Pearson Education.

24 Vioux A, Bideau JL, Mutin PH, Leclercq D (2004) Hybrid Organic-Inorganic Materials Based on Organ phosphorus Derivatives. In: Majoral JP (ed.) New Aspects in Phosphorus Chemistry IV; Topics in Current Chemistry; Springer Berlin Heidelberg 145-174.

25 Eklund J, Bond, AM, Alden J, Compton RG (1999) Perspectives in Modern Voltammetry: Basic Concepts and Mechanistic Analysis. Adv. Phys Org Chem 32: 1-120.

26 Compton RG (1987) Electrode Kinetics: Reactions: Reactions; Elsevier.